Carcinogenesis, 2021, Vol. 42, No. 11, 1357–1369

https://doi.org/10.1093/carcin/bgab098
Advance Access publication October 17, 2021
Original Article

ORIGINAL ARTICLE

GNA14's interaction with RACK1 inhibits hepatocellular carcinoma progression through reducing MAPK/JNK and PI3K/AKT signaling pathway

Cong Xu[1,], Yi-Ming Li[1], Bo Sun[1], Fang-Jing Zhong[1] and Lian-Yue Yang[1,2,*]

[1]Liver Cancer Laboratory, Xiangya Hospital, Central South University, Changsha 410008, Hunan, China and [2]Department of Surgery, Xiangya Hospital, Central South University, Changsha 410008, Hunan, China

*To whom correspondence should be addressed. Tel: +86-(0)731-84327365; Fax: (0)731-84327618; Email: xiangya100years@sina.com

Abstract

Gαq subfamily proteins play critical roles in many biological functions including cardiovascular development, angiogenesis, and tumorigenesis of melanoma. However, the understanding of G Protein Subunit Alpha 14 (GNA14) in diseases, especially in cancers is limited. Here, we revealed that GNA14 was significantly low expression in Human hepatocellular carcinoma (HCC) samples. Low GNA14 expression was correlated with aggressive clinicopathological features. Moreover, the overall survival (OS) and disease-free survival (DFS) of high GNA14 expression HCC patients were much better than low GNA14 expression group. Lentivirus-mediated GNA14 knockdown significantly promoted the growth of liver cancer *in vitro* and *in vivo*. However, opposing results were observed when GNA14 is upregulated. Mechanistically, We identified receptor for activated C kinase 1 (RACK1) as a binding partner of GNA14 by co-immunoprecipitation and mass spectrometry (MS). Glutathione-S-transferase (GST) pull-down assay further verified the direct interaction between GNA14 and RACK1. RNA-Seq and loss- and gain-of-function assays also confirmed that GNA14 reduced the activity of both MAPK/JNK and PI3K/AKT signaling pathways through RACK1. GNA14 synergized with U73122 (PLC inhibitor) to enhance this effect. Further studies suggested that GNA14 potentially competed with protein kinase C (PKC) to bind with RACK1, consequently reducing the stability of PKC. Moreover, we also showed that GNA14'supression of p-AKT protein level depended on sufficient RACK1 expression. In conclusion, we indicated a different role of GNA14, which acted as a suppressor inhibiting liver cancer progression through MAPK/JNK and PI3K/AKT signaling pathways. Due to this, GNA14 served as a potentially valuable prognostic biomarker for liver cancer.

Received: May 30, 2021; **Revised:** September 27, 2021; **Accepted:** October 15, 2021

Graphical Abstract

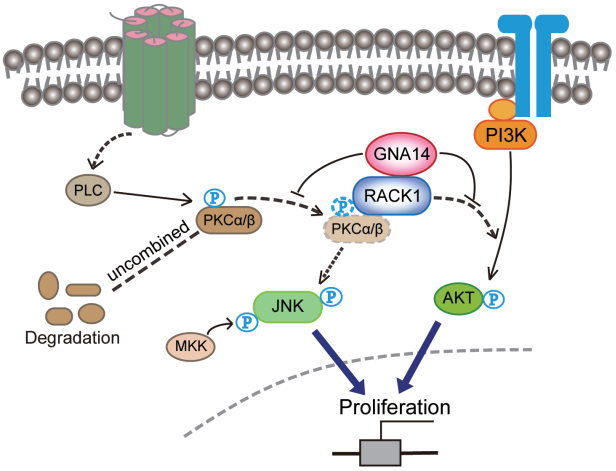

The schematic diagram of GNA14 inhibits PI3K/AKT and MAPK/JNK signaling pathway through combining with RACK1.

Abbreviations

DFS	disease-free survival
GNA11	G Protein Subunit Alpha 11
GNA14	G Protein Subunit Alpha 14
GNAQ	G Protein Subunit Alpha Q
GST	glutathione-S-transferase
HCC	hepatocellular carcinoma
OS	overall survival
PKC	protein kinase C
RACK1	receptor for activated C kinase 1

Introduction

Hepatocellular carcinoma (HCC), known to be the fourth leading cause of cancer-related death worldwide, led to a rough estimate of 841 000 new cases per year (1). HCC recurred in 70% of cases after surgical resection, a potentially curative treatment within 5 years. Unfortunately, there is no accepted neoadjuvant or adjuvant option to reduce the probability of recurrence currently (2–4). Therefore, the recurrence of HCC remains the biggest challenge for surgical therapy. In order to understand the mechanisms of HCC oncogenesis and identify key molecules that affect HCC, an increase of progression was urgently needed in order to set up the treatment target and improve the survival of HCC.

G protein-coupled receptors (GPCRs) are transmembrane proteins that transduce the chemical signals across the cell membrane and mediate the activation of intracellular G proteins (5). G proteins consist of three subunits, namely α, β, γ (6). According to sequence similarity and functional output, the Gα subunits have been divided into five different subfamilies (Gs, Gi, Gq, G12 and the newly discovered Gv). The Gq subfamily comprises four members. G Protein Subunit Alpha Q (GNAQ) and G Protein Subunit Alpha 11 (GNA11) are ubiquitously expressed; while G Protein Subunit Alpha 14 (GNA14) is found in kidney, liver, lung, and blood vessels, and GNA15/16 (mouse/human orthologues, respectively) is only expressed in hematopoietic cells (7).

Unlike GNA14, GNAQ and GNA11 are renowned for being commonly studied members of this subfamily. GNAQ and GNA11 have been unveiled to interact with more than 20 proteins which participate in many signaling pathways. In addition, GNAQ/11 specifically activates phospholipase C β (PLCβ) isozymes and initiates lipid- and calcium-dependent signaling pathways, such as JNK and ERK activity through Ras-dependent or Ras-independent mechanisms (8–10). Moreover, GNAQ/11 is also known as an inhibitor of PI3K/AKT signaling pathway. This is due to the direct and inhibitory effect of GTP-bound GNAQ/11 on p110α/p85α PI3K that competes with Ras, a PI3K activator (11,12). Furthermore, frequent GNAQ, GNA11, and GNA14 mutation has been known to be associated with vascular tumors and uveal melanoma (13–15). However, the understanding of GNA14 in diseases, in regards to cancer, is limited. Previous studies suggested that GNA14 was similar to GNAQ and GNA11 which stimulated downstream pathways through stimulating PLC or Ras (16,17). Wang et also reported that GNA14 silencing suppresses the proliferation and apoptosis in endometrial carcinoma cells (18). However, we observed that GNA14 expression frequently decreased in HCC and GNA14 low expression was an independent predictor for survival outcomes through statistic analysis of HCC samples from local patients. In regards to this, the conclusion was similar to the recent studies (19, 20). Moreover, Song et also reported that GNA14 regulated the RB pathway by promoting Notch1 cleavage to inhibit tumor proliferation, and might inhibit tumor metastasis by inhibiting the expression of JMJD6 (20). In this study, we also made it clear the role of GNA14 in inhibiting liver cancer growth through regulating PI3K/AKT and MAPK/JNK signaling pathways. These observations implied that in liver cancer, the role of GNA14 was potentially different from the understanding of Gαq subfamily we had known before.

Materials and methods

The samples and patients

One hundred and twenty HCC samples and one normal liver sample from a hepatic hemangioma patient were collected from January 2011 to December 2014. They were randomly selected from the Department of Surgery, Xiangya Hospital. Eighty HCC samples were collected from January 2011 to December 2014. They were randomly selected from the Department of Abdominal Surgical Oncology, Affiliated Cancer Hospital of Xiangya School of Medicine. The diagnosis of HCC patients was confirmed by two independent histopathologists. Follow-up procedures were

conducted as described in our previous study (21). Research protocols followed the Reporting Recommendations for Tumor Marker Prognostic Studies (REMARK) recommendations for reporting prognostic biomarkers in cancer (22).

Mouse models

Six-week-old male BALB/c nude mice were used for *in vivo* experiments. About 5 × 10^6 of HCC cells were injected subcutaneously into the right upper flank regions of BALB/c nude mice (n = 5 per group). The protocols of subcutaneous xenograft and orthotopic xenograft models followed the previous study (21). Six weeks later, the mice were sacrificed, and the samples were harvested, imaged, and processed for histopathological examination.

Ethics statement

The researches on human materials were approved by the ethics committee of Xiangya Hospital of Central South University and Affiliated Cancer Hospital of Xiangya School of Medicine, respectively. This study was conducted in compliance with the declaration of Helsinki. Written informed consent was obtained for the human studies. All *in vivo* murine experiments were approved by the Animal Ethics Committee of the Central South University.

Data mining

TCGA hepatocellular carcinoma samples, including normal and tumor samples, were downloaded from GDC Data Portal (https://portal.gdc.cancer.gov). GSE62232 data were downloaded from NCBI-GEO database (https://www.ncbi.nlm.nih.gov/geo/query/acc.cgi?acc=GSE62232).

Cell lines, cell culture and establishment of lentiviral transfected cells

Human liver cancer cell lines, Hep3B (RRID: CVCL_0326), PLC/PRF5 (RRID: CVCL_0485), and HepG2 (RRID: CVCL_0027) cell lines were purchased from the American Type Culture Collection (ATCC, Manassas, VA). MHCC97-L (RRID: CVCL_4973) and MHCC97-H (RRID: CVCL_4972) were given from the Liver Cancer Institute of Fudan University, Shanghai, China. L02 (RRID: CVCL_6926) and Huh7 (RRID: CVCL_0336) were purchased from the Cell Bank of Typical Culture Preservation Committee of Chinese Academy of Science (China). Cell culture medium was mixed with DMEM (high glucose with Glutamax, Biological Industries, Israel), antibiotics, and 10% FBS (Biological Industries Cat# 04-001-1A). Cells were cultured following the manufacturer's protocol. All human cell lines have been authenticated using short tandem repeat profiling within the last three years. All experiments were performed with mycoplasma-free cells.

The ectopic expression, downregulation lentivirus, and control lentivirus for GNA14 (Carrying purinomycin resistance) and receptor for activated C kinase 1 (RACK1) (Carrying hygromycin resistance) were purchased from Vigene Bioscience (China). Transfection was performed following the manufacturer's protocol. Puromycin (2 μg/ml) and hygromycin (200 μg/ml) were used to select stable clones. The shRNA and cDNA clones used in this study are listed in Supplementary Table S5, available at *Carcinogenesis* Online.

Quantitative real-time polymerase chain reaction

Quantitative real-time polymerase chain reaction (qRT-PCR) assay was performed as described in our previous study (21). GAPDH was used as normal control. All experiments were repeated 3 times. Sangon Biotech (China) synthesized the primers; the primer sequences are listed in Supplementary Table S3, available at *Carcinogenesis* Online.

Protein extraction and western blot

The protocols of protein extraction and western blot were followed as our previous study (21). The antibodies used are listed in Supplementary Table S4, available at *Carcinogenesis* Online.

Immunohistochemistry

Immunohistochemical (IHC) experiments were conducted as previously described (21). The antibodies used are listed in Supplementary Table S5, available at *Carcinogenesis* Online. IHC scores were calculated as described in previous study (23).

Immunocytochemistry

HCC cells were planked on glass slides. After 24 h, the cells were 4% paraformaldehyde in phosphate-buffered saline with 0.2% TritonX-100 (Solarbio Science, China). The other steps were the same as immunohistochemical.

RNA-sequencing and KEGG analysis

Hep3B-Vector and Hep3B-GNA14 cell lines were used for RNA-sequencing analysis. Cells were washed with cold PBS and total RNA was extracted with the mirVana miRNA Isolation Kit (Ambion). RNA integrity was evaluated with Agilent 2100 Bioanalyzer (Agilent Technologies, Santa Clara, CA). The samples with RNA Integrity Number (RIN) ≥7 were performed to the subsequent analysis. The libraries were constructed using TruSeq Stranded mRNA LTSample Prep Kit (Illumina, San Diego, CA) following the manufacturer's protocol. Then the libraries were sequenced on Illumina sequencing platform (HiSeqTM 2500 or Illumina HiSeq X Ten) and 125 bp/150 bp paired-end reads were generated by Shanghai OE Biotech. Co. Ltd. Raw data were processed with Trimmomatic. The reads were removed to obtain the clean reads. Then the clean reads were mapped to reference genome using hisat2. FPKM and read counts value of each transcript (protein_coding) were calculated using bowtie2 and eXpress. The original data was uploaded to the BioProject ID: PRJNA682449 (https://submit.ncbi.nlm.nih.gov/subs/bioproject/SUB8682868/overview). Differentially expressed genes (DEGs) were identified using the DESeq R package functions estimateSizeFactors and nbinomTest. *P value* <0.05 and fold Change >2 or fold Change <0.5 was set as the threshold for significantly differential expression. KEGG pathway enrichment analysis of DEGs was, respectively, performed using R based on the hypergeometric distribution.

Cignal finder cancer 10-pathway reporter arrays

A Cignal Finder 10-Pathway Reporter Array (SABiosciences, Valencia, CA) was used to detect the signaling pathways which were mediated by GNA14 in cell lines. The assay was conducted according to the manufacturer's protocol. Experiments were repeated 3 times.

Co-immunoprecipitation assay

Co-immunoprecipitation was performed with a Thermo Scientific Pierce co-immunoprecipitation kit (Rockford) following the manufacturer's instructions. The cells were treated with TPA (200 nM) and MG132 (20 μM) for 30 min. The cells were collected and lysed. AminoLink Plus coupling resins were incubated with the cell lysates overnight. GNA14 or RACK1 antibody was immobilized for 2 h with mixing AminoLink Plus coupling resin. Then the resins were washed, and the protein was eluted by using elution buffer. IgG as a negative control. Then, samples were analyzed by Western blot. The reagents used are listed in Supplementary Table S6, available at *Carcinogenesis* Online.

Protein identification using mass spectrometry

The cells were collected and lysed, GNA14 antibody was incubated with whole-cell lysates overnight. IP was performed as described above. Samples were run on SDS-Gel and stained with Coomassie Blue for 2 h before destaining in 5% MeOH, 7.5% HOAC, 87.5% H_2O. Excised gel bands were cut into 1 mm^3 pieces. Gel pieces were then subjected to a modified in-gel trypsin digestion procedure. Gel pieces were washed and dehydrated with acetonitrile for 10 min followed by acetonitrile removal. Then the enzymatic hydrolysates were analyzed by LTQ Orbitrap Velos Pro (Thermo Scientific).

Glutathione-S-transferase pull-down assays

Glutathione-S-transferase (GST) or GST-fusion proteins were expressed and purified, according to the manufacturer's instructions (Amersham Biosciences, England). *In vitro*-translated His-RACK1 was incubated with GST or GST-GNA14 bound to glutathione-Sepharose beads (Amersham Biosciences, England), and the adsorbed proteins were analyzed by

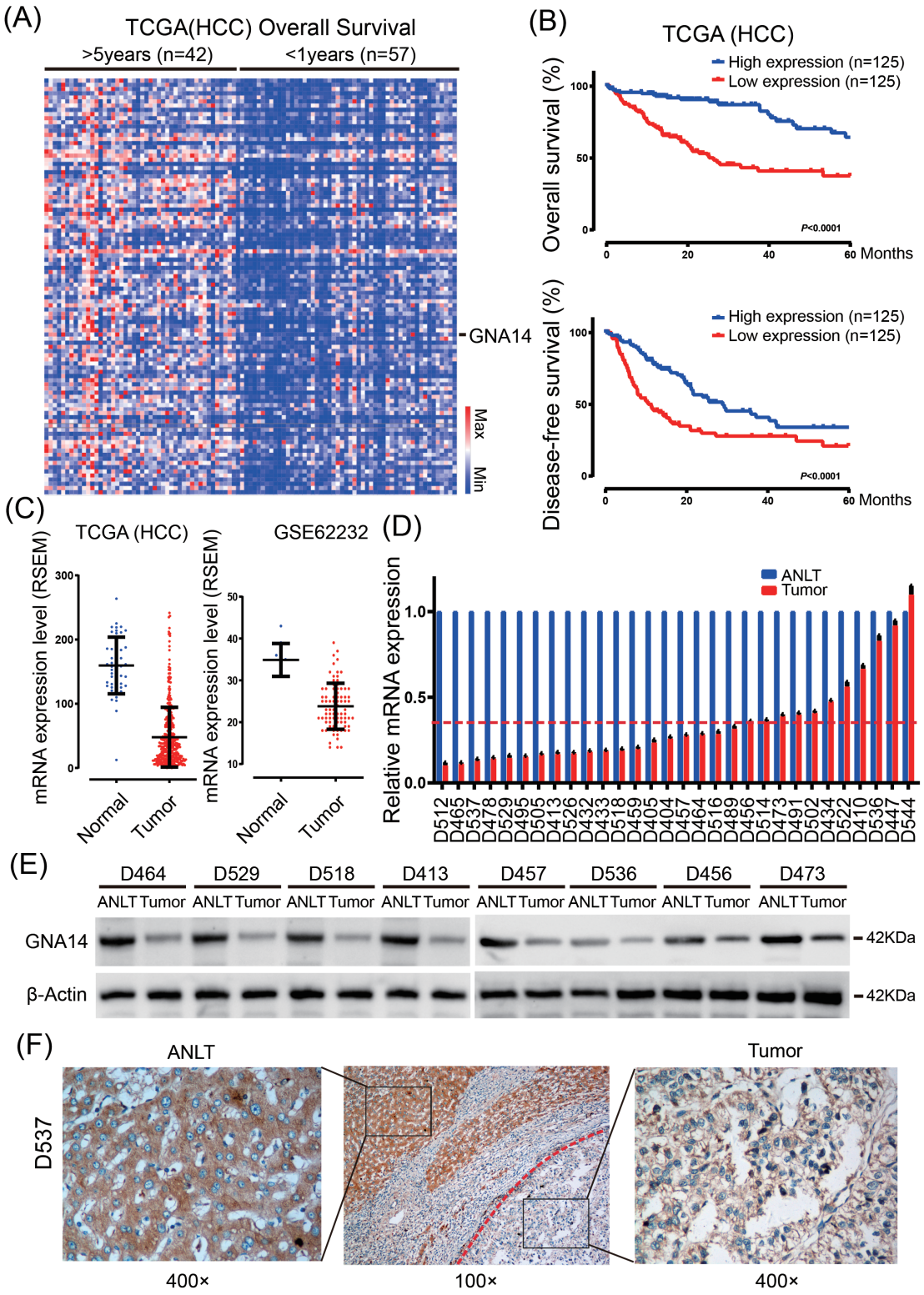

Figure 1. GNA14 expression was significantly decreased and associated with poor prognosis in HCC. (A) Heat map of the differentially expressed mRNA among 42 patients whose overall survival longer than 5 years and 57 patients shorter than 1 years based on TCGA-HCC data. Each row represents a gene and each column represents a sample. (B) Kaplan–Meier curves for overall survival and disease-free survival according to GNA14 expression by using TCGA-HCC data. (C) GNA14 expression was assessed in HCC tissues compared with normal tissues based on TCGA-HCC data (left) and GSE62232 (right). (D) GNA14 mRNA level was detected in 30 pairs HCC tissues and their adjacent non-tumor liver tissues (ANLT) by real-time PCR, imaginary line indicated the mean fold change. (E) 8 of the 30 pairs HCC tissues and their ANLTs were selected randomly and GNA14 expression was detected by western blot. (F) Representative IHC images of GNA14 expression also showed that GNA14 expression was lower in tumor tissues (right) than in ANLTs (left). The red broken line showed the border of the HCC tumor tissue. magnification: 100× (middle), 400× (left, right).

immunoblotting analysis. *In vitro*-translation kit was purchased from Promega (Wisconsin, USA).

Protein kinase C activity measurements

Protein kinase C (PKC) activity was investigated in crude membrane preparations by using the PepTag non-radioactive PKC assay (Promega, Wisconsin, USA) according to manufacturer's protocol.

Cycloheximide chase assay

A cycloheximide chase assay was used to determine the half-lives of PKC. Cells with aberrant GNA14 and/or RACK1 expression were treated with TPA (200 nM, 30 min) and cycloheximide (10 μg/ml) for the indicated times. The cells were lysed, and followed the subsequent experiments.

MTT assay, colony formation assay and cell cycle analysis

MTT assay and colony formation assay were followed the protocols described in previous work (21). For cell cycle analysis, 5×10^5 cells were incubated in 6-well plates for 24 h. The cells were fixed with cold 70% ethanol at –20°C overnight. The cells were stained in a solution containing PI (0.5 mg/ml) and RNase A (10 mg/ml) after washing with PBS. Then the cells were analyzed by FACS caliber flow cytometer (BD Biosciences, San Jose, CA), following quantification with FlowJo.v10 software. The experiments were performed in triplicate.

Statistical analysis

Statistical analyses were performed using SPSS 19.0 software (SPSS Inc., Chicago, IL) and GraphPad Prism 8. Data are presented as the mean ± SD from three repeated experiments.

Results

GNA14 is frequently low expression and predicts poor prognosis in HCC

TCGA-LIHC data included 377 RNA-sequencing data and matching clinical data of HCC patients. We have first chosen 99 patients and their matching data by considering prognosis after curative resection. We then divided into two subgroup; 42 patients whose overall survival (OS) longer than 5 years and 57 patients shorter than 1 year. While comparing the RNA-sequencing data of the two subgroups (Figure 1A) and GNA14 mRNA expression was significantly decreased in the substandard prognosticate subgroup ($P < 0.001$). The OS and disease-free survival (DFS) curves showed that 1/3 of total patients ($n = 125$) with the highest GNA14 mRNA expression had a significant longer OS ($P < 0.001$) and DFS ($P < 0.001$) than 1/3 of total patients ($n = 125$) with lowest GNA14 mRNA expression (Figure 1B). Moreover, GNA14 mRNA expression was lower in HCC tissues than that in normal liver tissues (Figure 1C). To further confirm it, we investigated GNA14 mRNA and protein level in randomly selected fresh HCC and adjacent non-tumor liver tissues (ANLT) from local HCC patients. As shown in Figure 1D–E, the relative mRNA (Mean 0.34 vs. 1.00, $P < 0.001$) and protein level of GNA14 was significantly lower in HCC samples compared with their matched ANLT. In addition, immunohistochemistry (IHC) assay also showed that GNA14 was poorly expressed in HCC, but excelled in expressing in adjacent-tumor liver tissues (Figure 1F).

To analyze the association between GNA14 expression and clinicopathological features of HCC patients, we selected 120 HCC patients as training cohort and 80 patients as validation cohort. We then divided the HCC patients into high GNA14 expression group (IHC score ≧ 4) and low GNA14 expression group (IHC score < 4) according to their GNA14 protein level in tumor samples. The representative IHC images of GNA14 high expression and low expression in HCC tumor samples were shown in Figure 2A. The 5-year OS (high vs. low 40.0% vs. 21.1%, $P < 0.001$) and DFS (high vs. low 32.5% vs. 18.9%, $P < 0.001$) in training cohort were much worse in low GNA14 expression group than in high GNA14 expression group (Figure 2B and D). As shown in Supplementary Table S1, available at *Carcinogenesis* Online, the low GNA14 expression in HCC was associated with adverse clinicopathological features like tumor size ($P < 0.001$), vascular invasion ($P = 0.019$), Barcelona Clinic Liver Cancer stage ($P < 0.001$) and tumor node metastasis stage ($P = 0.034$). Furthermore, the low GNA14 expression in HCC was an independent risk factor for both OS (95% CI, 1.168–2.699, $P = 0.009$) and DFS (95% CI, 1.267–3.628, $P = 0.007$) of HCC patients after liver resection in multivariate analysis (Figure 2C and E). The impact of GNA14 expression on HCC prognosis was further verified in the validation cohort (Figure 2F–I, Supplementary Table S2, available at *Carcinogenesis* Online).

GNA14 inhibits the growth of liver cancer *in vitro* and *in vivo*

To further study the role of GNA14 *in vitro* and *in vivo*. We firstly evaluated the protein level of GNA14 in human liver cancer cell lines, normal liver cell lines, and normal liver tissues (NLT) (Figure 3A). In addition, we downregulated GNA14 expression in Huh7 cells with high GNA14 expression and upregulated GNA14 in Hep3B cells with low GNA14 expression through lentivirus transfection (Supplementary Figure S1A, available at *Carcinogenesis* Online). Then we investigated the effect of GNA14 on cell proliferation with immunocytochemistry (Ki-67 staining), clone formation assay, and MTT assay. The proliferation capacity of Huh7-Vector and Hep3B-GNA14 cell lines were significantly lower than that of Huh7-shGNA14-1/-2 and Hep3B-Vector cell lines (Figure 3B–D). According to the cell-cycle assay, overexpression GNA14 in Hep3B-GNA14 cell line resulted in more HCC cells being blocked in the G0/G1 phase, while downregulated GNA14 in Huh7-shGNA14 cells induced more cells into the S and G2 phase (Figure 3E). These results were consistent with Gene Set Enrichment Analysis using the TCGA (HCC) database which showed that GNA14 expression had negative correlation with proliferation-associated pathways such as mitotic spindle pathway, MYC targets, and E2F target pathways (Supplementary Figure S1B, available at *Carcinogenesis* Online). We also investigated the effect of GNA14 in invasion or migration ability through transwell assay and wound-healing assay. However, compared with the effect of GNA14 on proliferation, the results were not exciting enough, although we observed the statistics differences between Huh7-Vector, Hep3B-Vector, and their GNA14-intervened cell lines (Supplementary Figure S1C and D, available at *Carcinogenesis* Online). To study the role of GNA14 *in vivo*, we established subcutaneous xenograft tumor models in nude mice as described previously (21). We then had to harvest the tumors 4 weeks after implantation (Figure 3D). Huh7-Vector cell-derived tumors at the subcutaneous implantation sites were significantly smaller with the growth rate lower than those of Huh7-shGNA14-1 and Huh7-shGNA14-2 cell-derived tumors; whereas Hep3B-Vector cell-derived tumors were significantly larger with the growth rate much faster than that of Hep3B-GNA14 cell-derived xenograft tumors. To mimic the liver environment and evaluate the role of GNA14 in the growth of liver cancer, we established orthotopic xenograft tumor models and inspected the orthotopic xenograft tumors 8 weeks after liver implantation. We later found much smaller tumors in the cell lines with high GNA14 expression in liver, suggesting GNA14's inhibition of *in vivo* tumor growth (Figure 3E). Subsequently, more Ki67 positive cells were found

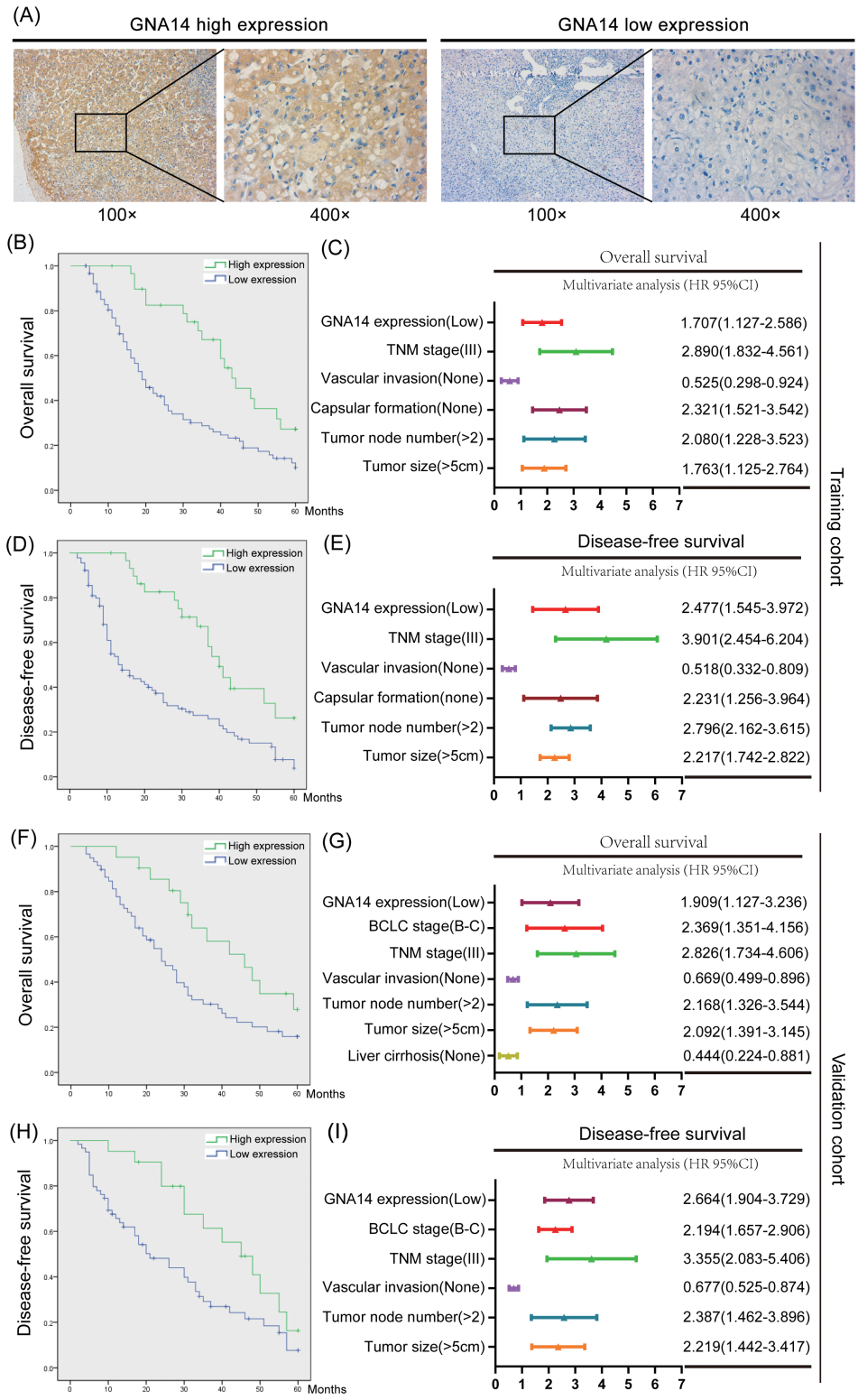

Figure 2. Low expression of GNA14 predicts poor prognosis in HCC patients. (A) Representative IHC images of GNA14 high expression and low expression in HCC tumor samples. (B) Kaplan–Meier curves for OS according to GNA14 expression. (C) Multivariate analysis of hazard ratios for OS in the training cohort (n = 120). (D) Kaplan–Meier curves for DFS according to GNA14 expression. (E) Multivariate analysis of hazard ratios for DFS in the training cohort (n = 120). (F) Kaplan–Meier curves for OS according to GNA14 expression. (G) Multivariate analysis of hazard ratios for OS in the validation cohort (n = 80). (H) Kaplan–Meier curves for DFS according to GNA14 expression. (I) Multivariate analysis of hazard ratios for DFS in the validation cohort (n = 80). *** $P < 0.001$.

in Huh7-shGNA14-1, Huh7-shGNA14-2, and Hep3B-Vector cell-derived orthotopic tumor than in Huh7-Vector and Hep3B-GNA14 (Figure 3F) after sectioning and staining the liver orthotopic xenograft tumors by Ki67. The information in the data has suggested that GNA14 inhibited liver cancer growth *in vivo* and *in vivo*.

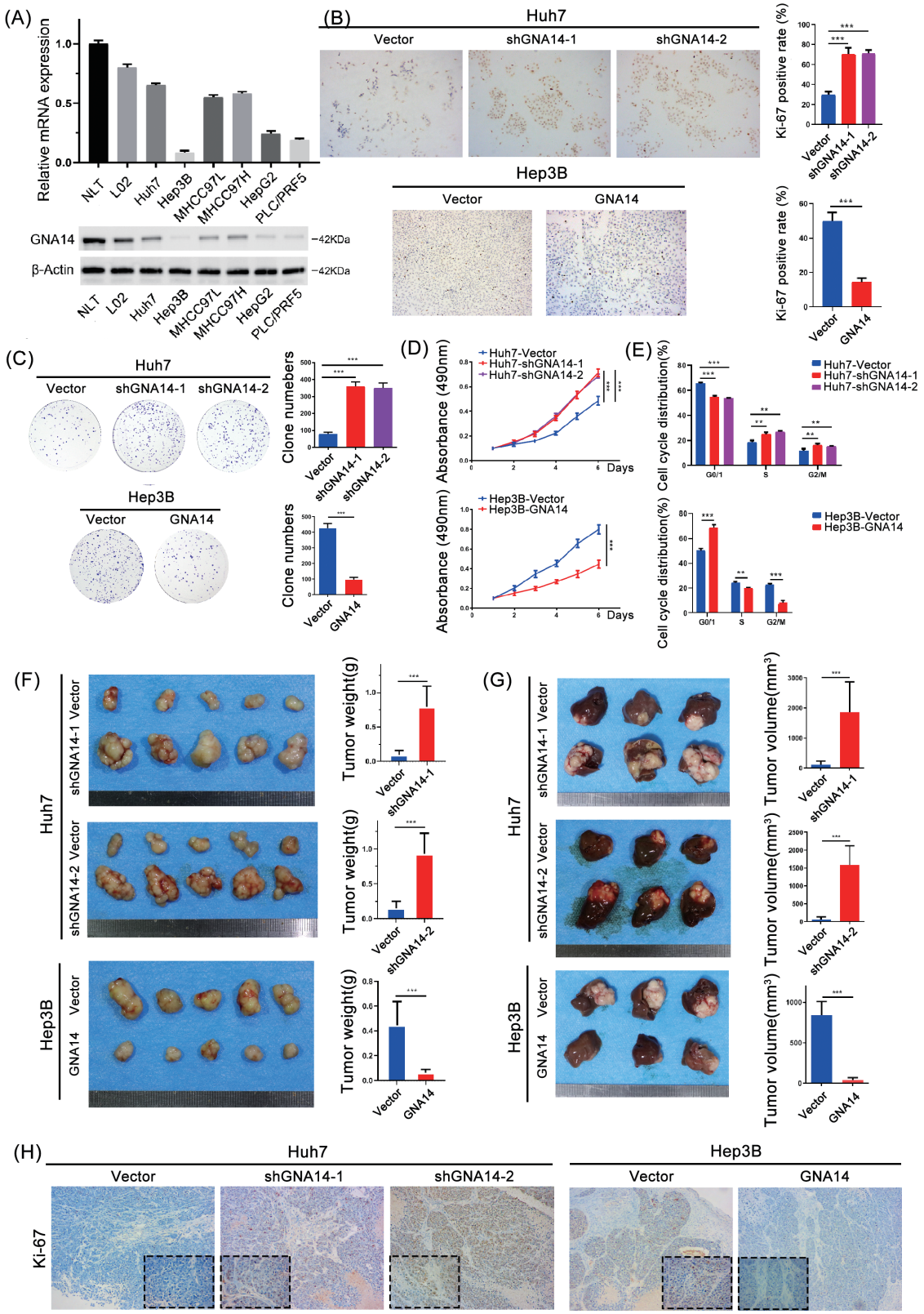

Figure 3. GNA14 inhibits the growth of liver cancer *in vitro* and *in vivo*. (A) GNA14 expression was investigated in normal liver tissues and liver cancer cell lines analyzed by real-time PCR and western blot. (B) Representative images of Ki67 staining in Huh7-shGNA14-1, Huh7-shGNA14-2, Hep3B-GNA14 cell ines and their control cells were shown. The histograms showed the percent of Ki-67 positive rate in each cell lines respectively. (C) The proliferation ability of GNA14-intervened Huh7 and Hep3B cell lines was monitored by colony formation assay. Representative micrographs (left) and quantifications (right) of liver cancer cell colonies in indicated cell lines. (D) MTT analysis of the proliferation ability of Huh7 and Hep3B transfectants. (E) DNA-content staining based cell-cycle analysis in GNA14-intervened Huh7 and Hep3B cell lines. DNA was stained by Propidium iodide. (F) Subcutaneous xenograft tumors from Huh7-shGNA14-1, Huh7-shGNA14-2 and Hep3B-GNA14 cells and their control

GNA14 inhibits PI3K/AKT and MAPK/JNK signaling pathway

Next, we conducted RNA-seq analysis on Hep3B-Vector and Hep3B-GNA14 cell lines to identify the pathway mechanism of GNA14 in liver cancer cells. We found that 1374 genes were differentially expressed (*Pval* < 0.05, *Padj* < 0.05), including 349 genes with absolute $\log_2$ (fold change) >2 (215 upregulated genes and 134 downregulated genes) (Supplementary Figure S1E, Supplementary Table S7, available at *Carcinogenesis* Online). As shown in further KEGG analysis, GNA14 inhibited the transcriptional activity of pathways in cancer [$-\log_{10}$ (*Pval*) = 4.54, List Hits = 49], PI3K-AKT [$-\log_{10}$ (*Pval*) = 3.23, List Hits = 35] and MAPK [$-\log_{10}$ (*Pval*) = 2.76, List Hits = 29] signaling pathways with list hits exceeding 25 (Figure 4A). According to Cignal Finder Cancer 10-Pathway Reporter Array-based dual-luciferase reporter system, GNA14 inhibited the transcriptional activity of MAPK/JNK signaling pathway (Figure 4B). It was further indicated in western blotting assay that the protein level of p-AKT and p-JNK in Hep3B cell lines were significantly reduced by ectopic GNA14 expression, while p-AKT and p-JNK protein levels were increased in GNA14 downregulated Huh7 cell line (Figure 4C). To further confirm it, we treated the HCC cell lines with or without MK2206 (AKT inhibitor, 1 μM, 24 h), SP600125 (JNK inhibitor, 10 μM, 24h). The results showed that downregulation GNA14 did not reverse the suppression of MK2206, SP600125 (Figure 4D). These suggested that JNK, AKT, and PKC were the downstream factors of GNA14. Consistently, it was revealed that high GNA14 expression was associated with low activity of AKT and JNK by IHC for orthotopic liver tumors' consecutive sections (Figure 4E). However, we didn't observe a significant change of p-ERK1/2 protein level in GNA14-intervened liver cancer cell lines. The results that came back implied that GNA14 played a different role from what we knew before in HCC. From above, we suggested that GNA14 inhibited liver cancer progression by suppressing PI3K/AKT and MAPK/JNK signaling pathways.

GNA14 inhibits the proliferation of liver cancer cells through interacting with RACK1

To define the GNA14 interactome, we conducted immunoprecipitation (IP) with an anti-GNA14 antibody from lysates of Hep3B-GNA14 cell lines. Proteins were then later separated on sodium dodecyl sulfate–polyacrylamide gel electrophoresis and identified by mass spectrometry (Supplementary Table S8, available at *Carcinogenesis* Online). Later, we identified RACK1 as a main protein interacting with GNA14 by mass spectrometry (Figure 5A). Additionally, previous studies suggested that RACK1 was involved in regulation of PI3K/AKT and MAPK/JNK signaling pathway (24–26). which was why we focused on RACK1 as the key factor. The potential interaction of GNA14 and RACK1 was confirmed by co-immunoprecipitation assay in Hep3B-GNA14 and Huh7-Vector cell lines (Figure 5B). Furthermore, GST pull-down assay showed the direct interaction between GNA14 and RACK1 (Figure 5C).

We established Huh7-shRACK1, Huh7-shGNA14-shRACK1, Hep3B-RACK1, and Hep3B-GNA14-RACK1 cell lines through lentivirus transfection. The infection efficiency was inspected respectively by western blotting and qRT-PCR (Figure 5D, Supplementary Figure S1F, available at *Carcinogenesis* Online). We conducted immunocytochemistry (Ki-67 staining), clone formation, MTT assay, and cell-cycle assay further to evaluate the proliferation capacity in not only Huh7, Hep3B, but also in their GNA14- and RACK1-intervened cell lines. The results showed that RACK1 severed as an oncogene to enhance the proliferation capacity of liver cancer cell lines, meanwhile, downregulated GNA14 expression in Huh7 cell lines reversed the effects of RACK1 on cell proliferation. The opposite observations were shown in Hep3B and its GNA14- and/or RACK1-intervened cell lines (Figure 5E–H).

GNA14 inhibits the activity of AKT and PKC induced by RACK1

Previous studies have shown that GNA14 was ligated to PLC activation (16). To explore the impact of PLC inhibitor on the GNA14-induced signaling pathways and whether or not GNA14 inhibited PI3K/AKT and MAPK/JNK pathway through RACK1. We evaluated p-AKT, p-JNK, and total AKT and JNK protein level by western blotting respectively in Huh7, Hep3B, and their GNA14- and/or RACK1-intervened cell lines with or without U73122 (PLC inhibitor, 10 μM, 30 min). The results showed that ectopic RACK1 expression enhanced the activity of AKT and JNK in Hep3B-RACK1 cell line compared with Hep3B-Vector cell line, even though this effect could be counteracted by GNA14 overexpression in Hep3B-GNA14-RACK1 cell line. The opposite results were observed in Huh7-Vector, Huh7-shRACK1, and Huh7-shGNA14-shRACK1 cell lines (Figure 6A). Moreover, U73122 synergized with GNA14 and RACK1 downregulation to inhibit PI3K/AKT and MAPK/JNK pathway, but downregulated GNA14 or upregulated RACK1 did not reverse the impact of U73122. These suggested that GNA14 inhibited the activity of PI3K/AKT and MAPK/JNK signaling pathway which could be enhanced by RACK1 in liver cancer cell lines. As a result, GNA14 presented a reverse trend to GNAQ/11 in regulating MAPK/JNK signaling pathway. Hence, we tended to study the mechanism of GNA14-regulated activity of MAPK/JNK signaling pathway through RACK1. Previous studies suggested that RACK1 acted as a key factor binding and stabilizing activated PKC, thus directly stimulating MAPK/JNK signaling pathway (24,27,28). Therefore, we inferred that GNA14 inhibited MAPK/JNK signaling pathway by disturbing the process. We first investigated PKC enzyme activity respectively in Hep3B, Huh7, and their GNA14- and/or RACK1-intervened cell lines. The results suggested that ectopic GNA14 expression inhibited the activity of PKC and reversed the effect of RACK1 on enhancing PKC activity in Hep3B cell lines; whereas the opposite effects were shown in Huh7 cell lines (Figure 6B). Furthermore, downregulation GNA14 did not reverse the suppression of PKC activity caused by Go 8639 (PKC inhibitor) (Supplementary Figure S1G, available at *Carcinogenesis* Online). Afterwards, because of the sufficient protein level of RACK1,

cells were established in nude mice. Subcutaneous tumors from Huh7-shGNA14-1, Huh7-shGNA14-2 and Hep3B-GNA14 cells and their control cells were removed and shown (left). The histograms showed the weight and statistic analysis of subcutaneous tumors (right). (G) Orthotopic tumors were established using subcutaneous tumors and removed after 6 weeks and each of the indicated groups is shown (left). Tumor volumes of tumors were calculated according to the following equation: V (mm^3) = width^2 (mm^2) × length (mm)/2 and the histograms showed the statistic analysis of orthotopic tumors. ***P < 0.001 based on the Student's *t*-test. Error bars, standard deviation. (H) Representative images of Ki67 staining in tissue sections from orthotopic tumors were shown. magnification: 100×, inset magnification: 400×.

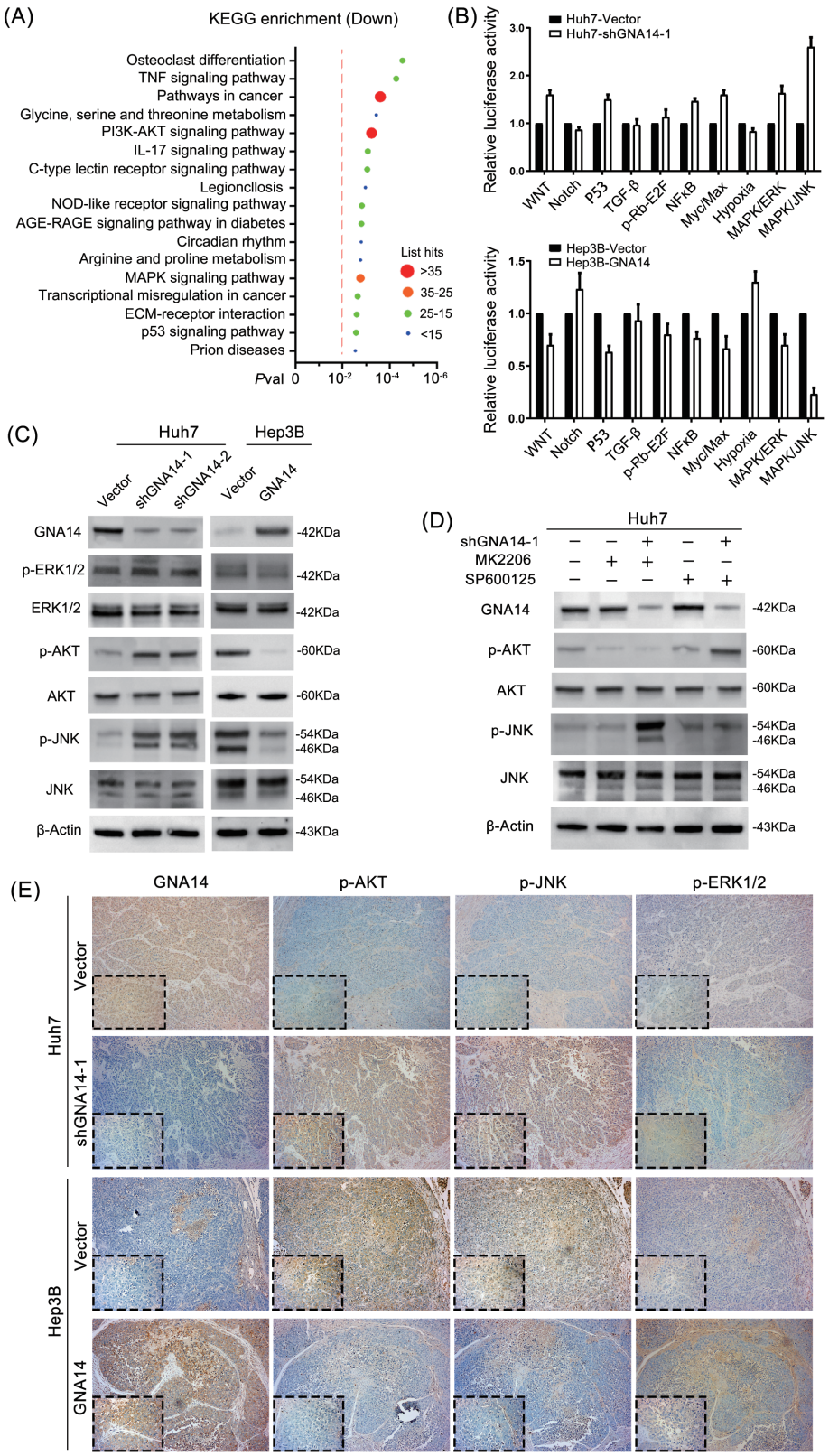

Figure 4. GNA14 inhibits PI3K/AKT and MAPK/JNK signaling pathway. (A) KEGG analysis was conducted to identify the downregulated pathways in Hep3B-GNA14 cell line by using RNA-seq data. Imaginary line indicated showed –log10(*Pval*) = 2. (B) The 10-Pathway Reporter Array showed the signaling change in GNA14-interfered cells. (C) The protein level of GNA14, the activity of JNK, AKT and ERK1/2 were detected by western blot using indicated antibodies. (D) Huh7-Vector and Huh7-shGNA14-1 cell lines were treated with MK2206 (1 μM, 24 h) or SP600125 (10 μM, 24 h). The protein level of p-AKT, p-JNK and other proteins were determined by western blot respectively. (E) Representative IHC images of GNA14, p-JNK, p-AKT and p-ERK1/2 protein level in orthotopic tumors serial slices. magnification: 100×, inset magnification: 400×.

we selected Huh7-Vector/Huh7-shGNA14 and Hep3B-RACK1/Hep3B-GNA14-RACK1 cell lines after treating with TPA (200 nM, 30 min), MG132 (20 μM, 30 min), and immunoprecipitated RACK1 from the lysates of these cell lines. We concluded investigating GNA14, RACK1, and PKCα/β protein level by western blotting that more GNA14 binding with RACK1 decreased the combination of

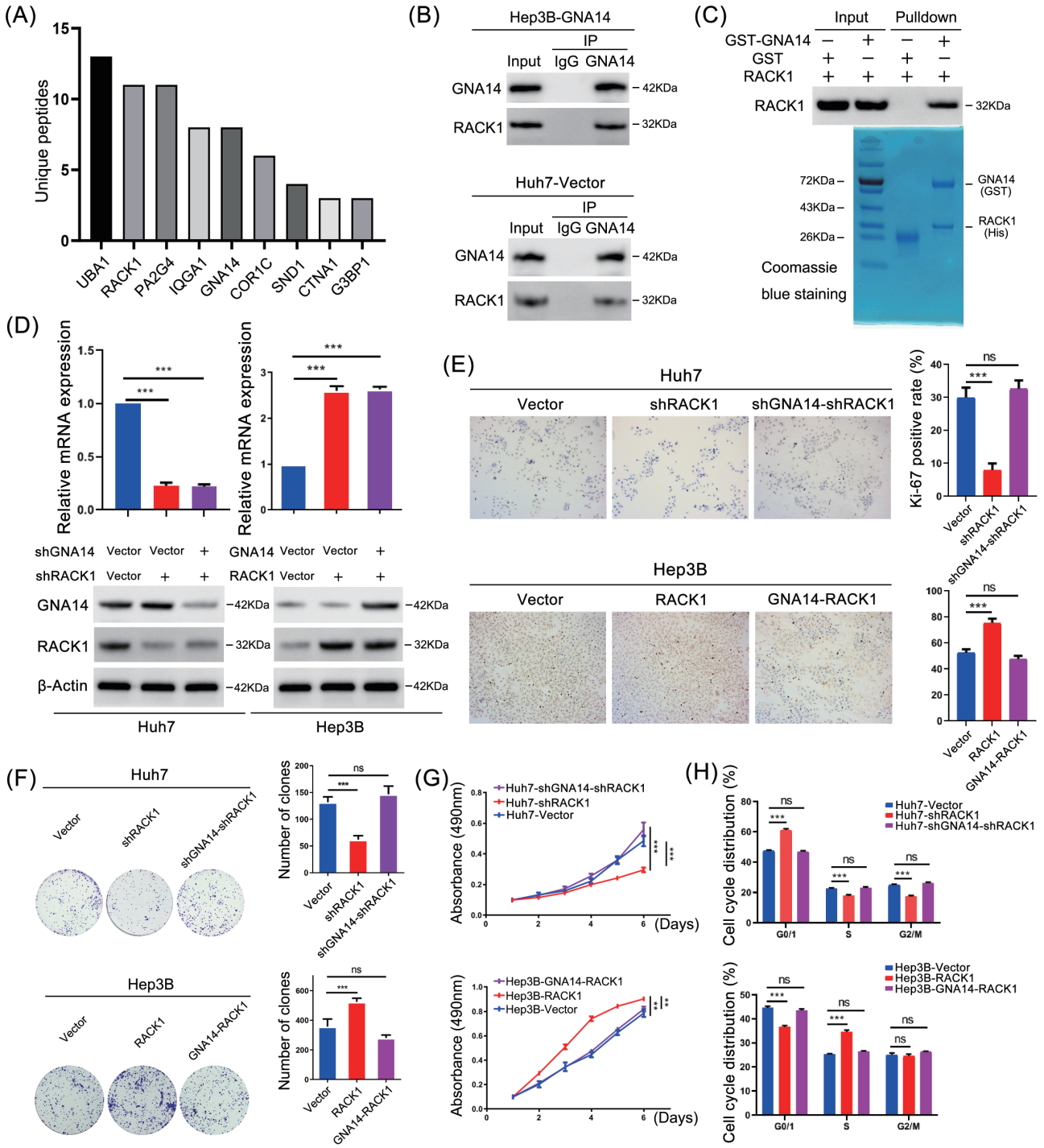

Figure 5. GNA14 inhibits the proliferation of liver cancer cells through interacting with RACK1. (A) Hep3B-GNA14 cells were lysed and incubated with anti-GNA14 antibody followed by mass spectrometry. The histograms showed the Unique Peptides of each protenin identified except cytoskeleton-associated proteins and nutrient metabolism proteins. (B) Hep3B-GNA14 and Huh7 cell were lysed and incubated with anti-GNA14 antibody followed by western blot assay with anti-RACK1 antibody and IgG as negative control. (C) GST and GST-tagged GNA14 were purified with glutathione agarose beads and incubated with His-RACK1. The membranes were detected with anti-RACK1 antibody. GST and the purified lysate were indicated in Coomassie Blue staining. (D) The protein level of GNA14 and RACK1 was determined by western blot respectively in GNA14/RACK1-intervened Huh7 and Hep3B cell lines. (E) Representative images of Ki67 staining in RACK1- and GNA14-intervened Huh7 and Hep3B cell lines were shown. The histograms showed the percent of Ki-67 positive rate in each cell lines respectively. (F) The proliferation ability of RACK1- and GNA14-intervened Huh7 and Hep3B cell lines was monitored by colony formation assay, MTT assay (G) and cell-cycle analysis, DNA was stained by Propidium iodide (H). *$P < 0.05$; **$P < 0.01$; ***$P < 0.001$ based on the Student's *t*-test. Error bars, standard deviation.

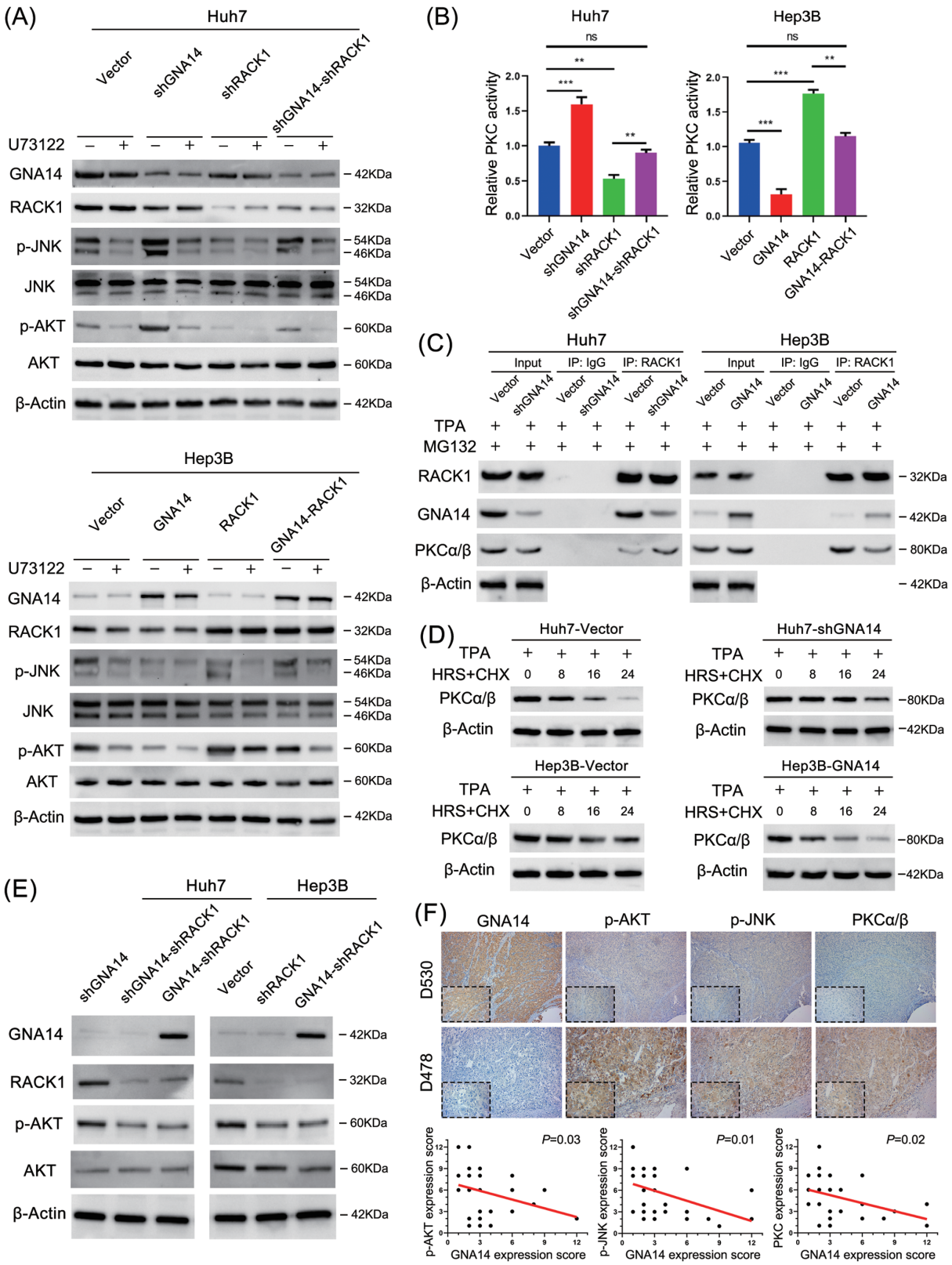

Figure 6. GNA14 inhibits the activity of AKT and PKC induced by RACK1. (A) The protein level of GNA14, p-JNK and p-AKT were detected by western blot using indicated antibodies in GNA14- and/or RACK1-intervened Huh7 and Hep3B cell lines after treating with or without U73122 (10 μM, 30 min). (B) PKC activity of GNA14- and/or RACK1-intervened Huh7 and Hep3B cell lines were measured by using a non-radioactive protein kinase C assay kit. Relative PKC activity in Huh7-Vector and Hep3B-Vector were taken as a control of 100%. Data shown are from three experiments. (C) Huh7, Hep3B and their lentivirus-infected cells were treated with TPA (200 nM) and MG132 (20 μM) for 30 min. Treated cells were collected, lysed, and used for RACK1 immunoprecipitation, followed by western blot analysis using the indicated antibodies. (D) Huh7, Hep3B and their lentivirus-infected cells were treated with TPA (200 nM, 30 min) and cycloheximide (10 μg/ml) at different time points as indicated followed by western blot analysis using the indicated antibodies. (E) The protein level of GNA14, RACK1 and p-AKT were detected by western blot using indicated antibodies in GNA14- and/or RACK1-intervened Huh7 and Hep3B cell lines. (F) Representative IHC images of GNA14, p-AKT, p-JNK and PKCα/β protein level in HCC serial slices. magnification: 100×, inset magnification: 400×. The correlation analysis between GNA14 and p-AKT, GNA14 and p-JNK, GNA14 and PKCα/β were shown in the diagram below.

RACK1 and PKCα/β in Hep3B cell line; in contrast, downregulated GNA14 in Huh7 cell line increased the combination of RACK1 and PKCα/β (Figure 6C). These suggested that GNA14 potentially competed and inhibited PKC via binding with RACK1. Then we investigated the steady-state level of PKCα/β in Hep3B, Huh7, and their GNA14-intervened cell line with TPA (200 nM, 30 min) and cycloheximide (10 μg/ml). The results later showed that PKC degradation efficiency increased in Hep3B-GNA14 cell line but decreased in Huh7-shGNA14 cell line (Figure 6D). Moreover, to further understand the mechanism that the interaction between GNA14 and RACK1 inhibited p-AKT protein level, we established Huh7-GNA14-shRACK1, Hep3B-shRACK1, and Hep3B-GNA14-shRACK1 cell lines. We investigated the p-AKT protein level in these cell lines respectively. The results showed that GNA14 overexpression could not reduce the p-AKT protein level again in Huh7-GNA14-shRACK1 and Hep3B-GNA14-shRACK1 cell lines (Figure 6E). These suggested that GNA14'supression of p-AKT depended on sufficient RACK1 expression. We randomly selected 30 from the 120 HCC patients previously mentioned, IHC assay for their HCC samples' consecutive sections showed that GNA14 expression was negative correlation with p-AKT, p-JNK and PKCα/β protein level (Figure 6F).

In general, we indicated that GNA14 inhibited liver cancer progression by reducing PI3K/AKT and MAPK/JNK signaling pathways. The direct interaction between GNA14 and RACK1 suppressed the activity of RACK1 which could have stimulated AKT activity and combined with PKC to activate JNK.

Discussion

Comparing the transcriptome expression differences between the better prognosticated HCC tissues and the poorer ones, we found an unexpected decrease in GNA14, encoding Gα14, in a poorly prognosticated group after comparing with the RNA-sequencing data of the two groups. As we know, G proteins are signal transducers transmitting the signal from the cell surface to the cell to activate downstream signaling pathways such as MAPK pathway (5,10). What's more, constitutive activation of the MAPK pathway (JNK/RAS/RAF/MEK/ERK) is common in liver cancer (29–31). Therefore, we were curious about the abnormal low expression of GNA14 in HCC tissues, especially in poorly prognosticated HCC tissues. Later studies have reported this. Tao et showed that downregulation of GNA14 in HCC indicated an unfavorable prognosis according to bioinformatic analysis of TCGA data (19). Song et also reported the same viewpoint. What's more, they confirmed the low expression of GNA14 in HCC through comparing the expression of GNA14 in HCC samples with normal liver samples (20). In this study, we not only verified that the low GNA14 expression in HCC was an independent risk factor for both OS and DFS of HCC patients, but also the low GNA14 expression in HCC was associated with adverse clinicopathological features like tumor size, vascular invasion, Barcelona Clinic Liver Cancer stage and tumor node metastasis stage. These all suggested that GNA14 potentially acted as a tumor suppressor in HCC.

Previous studies reported that GNA14 was ligated to the activity of Ras-dependent signaling pathways, like the other members of Gαq family (17,18). However, Song et reported that GNA14 regulated the RB pathway by promoting Notch1 cleavage to inhibit tumor proliferation, and might inhibit tumor metastasis by inhibiting the expression of JMJD6 (20). In this study, we also conducted an MS assay to find out the proteins interacting with GNA14. Although we did not identify the proteins like PLCβ, TRMP8, and p63RhoGEF that were unveiled to interact with GNAQ in previous studies (10,32,33), we later found that RACK1 was a key protein interacting with GNA14. These results implied a different role of GNA14 in liver cancer, despite being a member of Gαq family.

RACK1 has been suggested to act as a scaffolding protein, recruiting different factors to the ribosome, or recruiting the ribosome to various subcellular locations. RACK1 combined with and stabilized activated PKC to activate the downstream pathways, such as MAPK/JNK (24,27,28,34). Moreover, Src, β-integrin, and FAK are also found to interact with RACK1 (34–36). However, the role of RACK1 in cancers seems to depend on cancer types. RACK1 promotes the proliferation of HCC cells via interacting with PKC and/or MKK7 and enhances JNK signaling pathway (27). In esophageal carcinoma, RACK1 promotes proliferation and chemotherapy resistance by activating the PI3K/AKT pathway (26). Similar results are observed in lung cancer and THP1 acute myeloid leukemia cells (37,38). Contrary to this, RACK1 suppresses Wnt/β-catenin signaling and decreases tumorigenicity of gastric cancer cells through binding GSK3β and Axin and stabilizing the destruction complex (39). Our results confirmed the role of RAKC1 as an oncogene in HCC. We also found that the interaction between GNA14 and RACK1 prevented RACK1's combining with activated PKC. As a result, the interaction between GNA14 and RACK1 promoted the degradation of activated PKC and consequently inhibited MAPK/JNK signaling pathway. Here, we did not observe the change of p-ERK1/2 protein level. We thought that GNA14 may stimulate another pathway to activate ERK which was independent of PLC-PKC, such as TPR1-Ras-ERK pathway (7). As a whole, GNA14 did not regulate MAPK/ERK observably. Furthermore, the interaction between GNA14 and RACK1 suppressed the promoting effect of RACK1 on PI3K/AKT pathway in HCC. This process depended on sufficient RACK1 expression.

In conclusion, we showed a different role of GNA14 from the other Gαq members: GNA14 inhibited the growth of liver cancer and suppressed the activity of MAPK/JNK and PI3K/AKT signaling pathway through interaction with RACK1. Although GNA14 may not transmit stimulated signal to activate downstream pathways, it can act as an inhibitor to inhibit MAPK/JNK and PI3K/AKT signaling pathway in liver cancer. According to our results, Gαq subfamily may be more complex than we knew in cancers. Different members may act in different role in different cancer types. These observations suggested more dialectic needed to target Gq pathway in liver cancer clinic treatment.

Supplementary material

Supplementary data are available at *Carcinogenesis* online.

Funding

Key Project of the National Natural Science Foundation of China [grant number 81330057]; the National Natural Science Foundation of China [grant number 81773139]; the National Science and Technology Major Project [grant number 2017ZX10203207-002-003].

Acknowledgements

The authors thank Prof. Qiong-qiong He and Prof. Geng-Qiu Luo (Department of Pathology, Xiangya Hospital of Central South University) for the help of pathological diagnoses and guidance. The authors also thank Ivy Ly for the help of English checking and revision.

Conflict of Interest Statement: The authors declare no potential conflicts of interest.

Data availability

The raw RNA sequencing data are available in BioProject under accession number PRJNA682449. Other data that support the findings of this study are available from the corresponding author upon request.

References

1. Bray, F. *et al.* (2018) Global cancer statistics 2018: GLOBOCAN estimates of incidence and mortality worldwide for 36 cancers in 185 countries. *CA. Cancer J. Clin.,* 68, 394–424.
2. Forner, A. *et al.* (2018) Hepatocellular carcinoma. *Lancet,* 391, 1301–1314.
3. Vogel, A. *et al.* (2020) Current strategies for the treatment of intermediate and advanced hepatocellular carcinoma. *Cancer Treat. Rev.,* 82, 101946.
4. Finn, R.S. *et al.* (2018) Therapies for advanced stage hepatocellular carcinoma with macrovascular invasion or metastatic disease: a systematic review and meta-analysis. *Hepatology,* 67, 422–435.
5. Hepler, J.R. *et al.* (1992) G proteins. *Trends Biochem. Sci.,* 17, 383–387.
6. Cassel, D. *et al.* (1978) Mechanism of adenylate cyclase activation through the beta-adrenergic receptor: catecholamine-induced displacement of bound GDP by GTP. *Proc. Natl. Acad. Sci. U. S. A.,* 75, 4155–4159.
7. Sánchez-Fernández, G. *et al.* (2014) Gαq signalling: the new and the old. *Cell. Signal.,* 26, 833–848.
8. Lee, C.H. *et al.* (1992) Members of the Gq alpha subunit gene family activate phospholipase C beta isozymes. *J. Biol. Chem.,* 267, 16044–16047.
9. Smrcka, A.V. *et al.* (1993) Regulation of purified subtypes of phosphatidylinositol-specific phospholipase C beta by G protein alpha and beta gamma subunits. *J. Biol. Chem.,* 268, 9667–9674.
10. Faure, M. *et al.* (1994) cAMP and beta gamma subunits of heterotrimeric G proteins stimulate the mitogen-activated protein kinase pathway in COS-7 cells. *J. Biol. Chem.,* 269, 7851–7854.
11. Ballou, L.M. *et al.* (2000) Differential regulation of the phosphatidylinositol 3-kinase/Akt and p70 S6 kinase pathways by the alpha(1A)-adrenergic receptor in rat-1 fibroblasts. *J. Biol. Chem.,* 275, 4803–4809.
12. Ballou, L.M. *et al.* (2003) Activated G alpha q inhibits p110 alpha phosphatidylinositol 3-kinase and Akt. *J. Biol. Chem.*, 278, 23472–23479.
13. Couto, J.A. *et al.* (2017) A somatic GNA11 mutation is associated with extremity capillary malformation and overgrowth. *Angiogenesis,* 20, 303–306.
14. Lim, Y.H. *et al.* (2016) GNA14 somatic mutation causes congenital and sporadic vascular tumors by MAPK activation. *Am. J. Hum. Genet.,* 99, 443–450.
15. Chen, X. *et al.* (2017) RasGRP3 mediates MAPK pathway activation in GNAQ mutant uveal melanoma. *Cancer Cell.,* 31, 685–696.
16. Ho, M.K. *et al.* (2001) Galpha(14) links a variety of G(i)- and G(s)-coupled receptors to the stimulation of phospholipase C. *Br. J. Pharmacol.,* 132, 1431–1440.
17. Kwan, D.H.T. *et al.* (2012) Activation of Ras-dependent signaling pathways by G(14) -coupled receptors requires the adaptor protein TPR1. *J. Cell Biochem.,* 113, 3486–3497.
18. Wang, J. *et al.* (2018) GNA14 silencing suppresses the proliferation of endometrial carcinoma cells through inducing apoptosis and G2/M cell cycle arrest. *Biosci Rep.,* 38, BSR20180574.
19. Yu, T. *et al.* (2020) Downregulation of GNA14 in hepatocellular carcinoma indicates an unfavorable prognosis. *Oncol Lett.,* 20, 165–172.
20. Song, G. *et al.* (2021) Hypermethylation of GNA14 and its tumor-suppressive role in hepatitis B virus-related hepatocellular carcinoma. *Theranostics*, 11, 2318–2333.
21. Xiao, S. *et al.* (2016) Actin-like 6A predicts poor prognosis of hepatocellular carcinoma and promotes metastasis and epithelial-mesenchymal transition. *Hepatology,* 63, 1256–1271.
22. Sauerbrei, W. *et al.* (2018) Reporting Recommendations for Tumor Marker Prognostic Studies (REMARK): an abridged explanation and elaboration. *J. Natl. Cancer Inst.,* 110, 803–811.
23. Wang, Y. *et al.* (2014) ASPP2 controls epithelial plasticity and inhibits metastasis through beta-catenindependent regulation of ZEB1. *Nat. Cell Biol.,* 16, 1092–1104.
24. López-Bergami, P. *et al.* (2005) RACK1 mediates activation of JNK by protein kinase C [corrected]. *Mol. Cell,* 19, 309–320.
25. Kong, Q. *et al.* (2016) RACK1 is required for adipogenesis. *Am. J. Physiol. Cell Physiol.,* 311, C831–C836.
26. Liu, B. *et al.* (2018) RACKI induces chemotherapy resistance in esophageal carcinoma by upregulating the PI3K/AKT pathway and Bcl-2 expression. *Onco. Targets. Ther.,* 11, 211–220.
27. Guo, Y. *et al.* (2013) Receptor for activated C kinase 1 promotes hepatocellular carcinoma growth by enhancing mitogen-activated protein kinase kinase 7 activity. *Hepatology,* 57, 140–151.
28. Sharma, G. *et al.* (2013) Affinity grid-based cryo-EM of PKC binding to RACK1 on the ribosome. *J. Struct. Biol.*, 181, 190–194.
29. Chen, J. *et al.* (2015) ECT2 regulates the Rho/ERK signalling axis to promote early recurrence in human hepatocellular carcinoma. *J. Hepatol.*, 62, 1287–1295.
30. Lin, S. *et al.* (2017) Melatonin promotes sorafenib-induced apoptosis through synergistic activation of JNK/c-jun pathway in human hepatocellular carcinoma. *J. Pineal Res.,* 62. doi:10.1111/jpi.12398.
31. Han, T. *et al.* (2015) PTPN11/Shp2 over-expression enhances liver cancer progression and predicts poor prognosis of patients. *J. Hepatol.*, 63, 651–660.
32. Lutz, S. *et al.* (2007) Structure of Galphaq-p63RhoGEF-RhoA complex reveals a pathway for the activation of RhoA by GPCRs. *Science,* 318, 1923–1927.
33. Zhang, X. *et al.* (2012) Direct inhibition of the cold-activated TRPM8 ion channel by Gαq. *Nat. Cell Biol.*, 14, 851–858.
34. Ron, D. *et al.* (1994) Cloning of an intracellular receptor for protein kinase C: a homolog of the beta subunit of G proteins. *Proc. Natl. Acad. Sci. U. S. A.,* 91, 839–843.
35. Chang, B.Y. *et al.* (2002) RACK1: a novel substrate for the Src protein-tyrosine kinase. *Oncogene*, 21, 7619–7629.
36. Trerotola, M. *et al.* (2012) Trop-2 inhibits prostate cancer cell adhesion to fibronectin through the β1 integrin-RACK1 axis. *J. Cell Physiol.,* 227, 3670–3677.
37. Shi, S. *et al.* (2012) RACK1 promotes non-small-cell lung cancer tumorigenicity through activating sonic hedgehog signaling pathway. *J. Biol. Chem.*, 287, 7845–7858.
38. Zhang, D. *et al.* (2013) RACK1 promotes the proliferation of THP1 acute myeloid leukemia cells. *Mol. Cell Biochem,*. 384, 197–202.
39. Deng, Y.Z. *et al.* (2012) RACK1 suppresses gastric tumorigenesis by stabilizing the β-catenin destruction complex. *Gastroenterology*, 142, 812–823.e15.